UCRL-91411
PREPRINT

CONF-8408124--1

X-Ray Spectroscopy of Laser-Produced Plasmas

Robert L. Kauffman

This paper was prepared for submittal to
Proceedings of 8th International Colloquium on
EUV and X-ray Spectroscopy of Astrophysical and
Laboratory Plasmas
Washington, DC - August 27-29, 1984

August 1984

MASTER

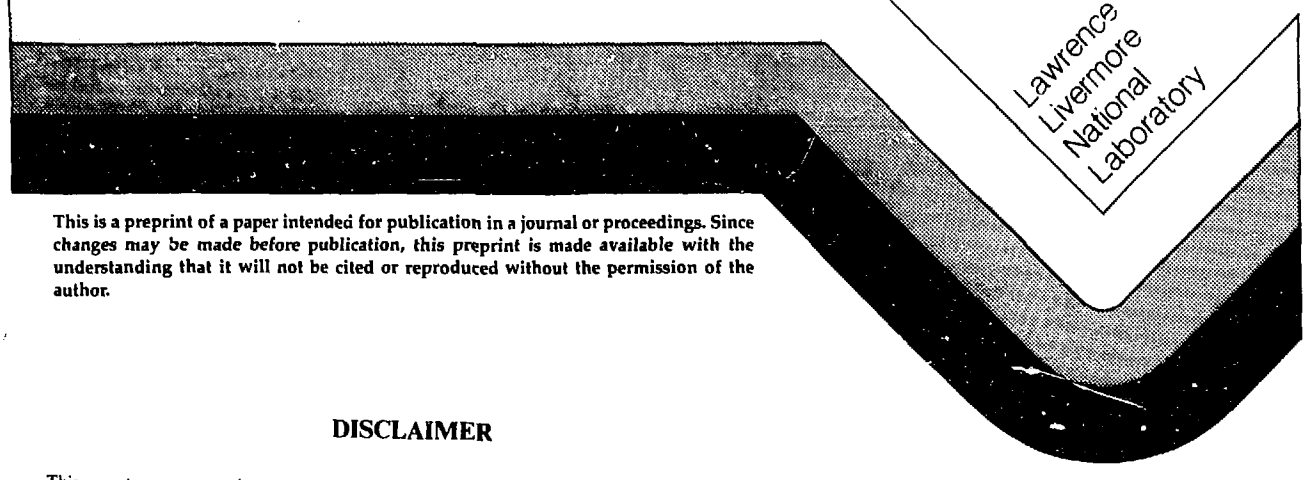

DISCLAIMER

DISTRIBUTION OF THIS DOCUMENT IS UNLIMITED

X-ray Spectroscopy of Laser-Produced Plasmas*

Robert L. Kauffman

Lawrence Livermore National Laboratory
Livermore, California 94550

UCRL--91411

DE85 002170

Laser-produced plasmas have some of the highest temperatures and densities obtainable in the laboratory. This offers the opportunity to perform spectroscopic studies in new temperature and density regimes under controlled laboratory conditions. Temperatures can range from greater than 1 keV to less than 1 eV, while densities range from less than $10^{20} e^-/cm^3$ to greater than $10^{23} e^-/cm^3$. X-ray spectroscopy has been an important tool in diagnosing these large ranges of temperature and density. Relative line intensities of resonance and satellite lines can be used to diagnose the lower densities and higher temperatures. (Galanti and Peacock 1975, Boilo et al. 1979) For the denser plasmas Stark broadening is a good density diagnostic. (Yaakobi et al. 1977) Absorption spectroscopy measuring edge shifts had recently been used to probe the low temperature, high density region. These plasmas, with their high-energy density, are transient with total time scales ranging from 100 psec to greater than 1 nsec, depending on the laser driver pulse. In order to make detailed measurements from these plasmas, sensitive, time-resolved spectrographs have been developed. (Lewis et al. 1980, Kauffman et al. 1983) These spectrographs can measure time histories of spectral lines with resolving powers of 300 or greater and with time-resolutions of 20 psec. By using such instruments, studies of the dynamics of the plasma can be made.

The laser-produced plasma can be divided into three different regions. The first is the corona region. This extends from critical density for light absorption [$10^{21} e^-/cm^3/\lambda^2(\mu m)$] to lower density. Temperatures can range from a few hundred eV to greater than one keV. In this region laser energy is deposited in the plasma. Not only is it characterized by high temperatures and low densities, but the light absorption can also create non-thermal electron distributions.

Spectroscopically the corona is the easiest part of the plasma to access. The high temperatures produce high brightnesses of highly stripped ions. Many of the x-ray diagnostics for the solar corona are directly applicable to this regime. Some of the major problems in interpreting the data are opacity, time-dependence, and spatial gradients. Because of the relatively high densities even in the corona, most resonance line intensities are many optical depths thick, unless care is taken to reduce these effects in the target. The time dependence and spatial gradients are a direct result of the finite time and localized area of laser energy deposition. This deposition creates large gradients, both into the cold dense material and laterally away from the deposition area. Also, as the plasma evolved the gradient scale lengths change.

One application of x-ray line intensities has been to measure the coronal temperature in a thin foil experiment. The purpose of the experiment is to create long-scalelength, underdense plasmas, such as may

*This work was performed under the auspices of the U.S. Department of Energy by Lawrence Livermore National Laboratory under contract No. W-7405-Eng-48.

be found in advanced ICF targets. The laser propagating in such plasmas can efficiently couple to electron-plasma waves, which produce high-energy electrons. The coupling efficiency depends on the plasma temperature and density. The underdense plasma was created by irradiating thin CH foils that expand during the heating to the desired density by the peak of the laser pulse. These foils are typically 1000 μm diameter and 2μm thick for irradiation by our Novette laser using 0.53 μm light. For spectroscopic purposes we have seeded only the inner 300 μm of the foil with 4% atomic concentration of Sulfur. The low concentration of the seed material was chosen in order not to effect the hydrodynamics of the foil and to reduce the opacity of the resonance lines. Only the center portion is seeded in order to minimize effects of lateral gradients as the heat spreads away from the initial spot.

Data from such an experiment is shown in Fig. 1. The data was taken using an x-ray streak camera coupled to an x-ray crystal spectrograph. (Kauffman et al. 1983) In the figure time increases upward and energy increases to the right. The time resolution is on the order of 20 psec and energy resolution is about 8eV. The sulfur helium-like and hydrogen-like lines are marked.

The relative intensity ratio of the Heα and Lyα lines from Fig. 1 are compared with calculations to obtain temperatures. This comparison is shown in Fig. 2. The calculations combine the output of a two-dimensional hydrodynamics code with a code that calculates the atomic levels dynamically. (R. W. Lee et al. 1984a) The atomic levels code uses the temperature and density of each cell derived from the hydrodynamics code and calculates the transient level populations of the sulfur at each time step. In this way effects on ionization balance due to step gradients are included. Results of this calculation are shown as the solid line in Fig. 2. The agreement with the data overall is good. Although early in the pulse during the times of steep gradients, it predicts too slow of ionization time. The dashed line is the prediction assuming the ion is in full steady-state with the local plasma parameters and the agreement is much better.

We have used other x-ray features to diagnose the corona. We have used Stark broadening of high n-state lines in the plasma to measure densities in Al plasmas down to $10^{20} e^-/cm^3$. (Lee et al. 1984b) We have also measured the time history free-bound continuum from Al plasmas. (Matthews et al. 1984) The shape of the continuum provided some indication of a non-thermal distribution during the laser heating and the plasma cooling rate after the laser was turned off. Both techniques require high concentrations of the spectroscopic ion and low background for accurate measurements.

The second region is the ablation/pusher region of the plasma. In this region energy is transferred from the corona to the inner fuel. This region is relatively dense and cool, but large thermal and density gradients can exist due to strong shocks propagating through it. Only recently has x-ray spectroscopy been applied to study the physics here, although it should receive more attention in the future. (Hares et al. 1984) have used absorption spectroscopy to measure edge shifts and widths to determine temperatures and densities of strong shocks inside of materials. Several groups have used inner-shell electron fluorescence to study electron conduction from the corona into the dense material region. (Young et al. 1977, Yaakobi et al. 1984)

The third region is the inner fuel or core of the implosion. This region remains relatively cool during the implosion, but once the center stagnates, the kinetic motion can be converted to thermal energy heating the fuel. By adding a high-Z seed gas to the D-T, spectroscopy can be used to measure the final compressed density, which is important for determining the quality of the implosion.

Line broadening data has been obtained by using the Omega laser at the University of Rochester to symmetrically irradiate the outer surface of an Ar-filled ball. The data have been fit using line broadening theory developed by C. Hooper and co-workers and opacity modeling by R. W. Lee. (Delameter et al. 1984) Opacity effects are important because they represent another broadening mechanism. Each line can be fit independently to a number of different electron densities, depending on the opacity. Fig. 3 shows the focus of best fit for each line versus the ion density in the hydrogen ground state, or optical depth. The intersection of all of the locii of best fit for each line uniquely determines both the electron density and the ion density for the implosion. Of special note is the importance of optically thick lines in the fitting procedure. These severely constrain the ion density and the region of interest for the fitting plot. The dotted lines in the figure indicate regions where 30% and 50% of the ions are in the hydrogen-like ground state. For more details, see the paper by Delameter et al. (1984).

In summary, x-ray spectroscopy is an important diagnostic tool for laser-produced plasmas. Experimental conditions, though, must be carefully tuned to obtain meaningful results. Of particular note, is the role of opacity and time dependence. Both must be included in any analysis of x-ray spectra from laser-produced plasmas.

References

Boiko, V. A., Pikuz, S. A., and Faenov, A. Ua., 1979 J. Phys. B, 12, 1989.

Delameter, N. D., Hooper, C. F., Joyce, R. F., Woltz, L. A., Ceglio, N. M., Kauffman, R. L., Lee, R. W., and Richardson, M. C., 1984, submitted to Phys. Rev. Lett., and J. Quant. Spec. Radiat. Transfer, to be published.

Galanti, M., and Peacock, N. J., 1975, J. Phys. B, 8, 2427.

Hares, J. D., Bradley, D. K., Ranking, H. J., and Rose, S. J., 1984,, Central Laser Facility Annual Report, Rutherford Laboratory, A3.1.

Kauffman, R. L., Brown, T., and Medecki, H., 1983, SPIE Vol. 427, 84.

Lee, R. W., Kilkenny, J. D., Kauffman, R. L., and Matthews, D. L., 1984b, J. Quant. Spectrosc. Radiat. Transfer, 31, 83.

Lee, R. W., Whitten, B. L., and Stout, R. E., II, 1984a, J. Quant. Spectrosc. Radiat. Transfer, 32, 91 (1984).

Lewis, C. L. S., Lamb, M. J., Kilkenny, J. D., Keats, S., and Key, M. H., 1980 Central Laser Facility Annual Report, Rutherford Laboratory, 61.

Matthews, D. L., Kauffman, R. L., Kilkenny, J. D., and Lee, R. W., 1984 Appl.. Phys. Lett 44 586.

Yaakobi, B. A., et al. 1984, Phys. Fluids 27, 516.

Yaakobi, B., Steel, D., Thorsos, E., Hauer, A., and Perry B., 1977, Phys. Rev. Lett., 39, 1526.

Young, F. C., Whitlock, R. R.,, Decoste, R., Ripin, B. H. Nagel, D. J. , Stamper, J. A., McMahon, J. M., and Bodner, S. E., 1977, Appl. Phys. Lett. 30, 45.

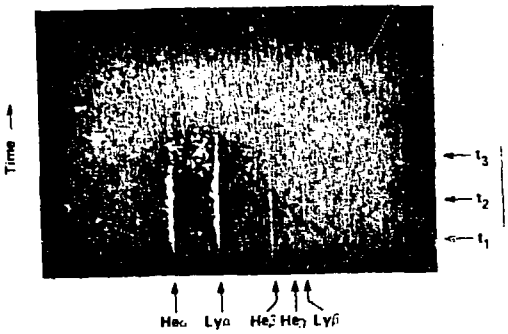

Fig. 1 Example of a time-resolved K-x-ray spectrum of Sulfur. The sulfur is a low concentration seed in CH. The relative line intensities are used to measure the time-resolved density and temperature of the foil.

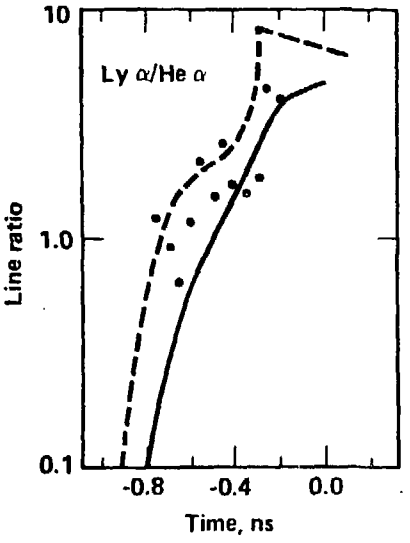

Fig. 2 Example of the time-resolved Lyα/Heα ratio of Sulfur from exploding foils. The solid and dashed curves are the predicted line ratio from a 2-d hydrodynamic code coupled with a dynamic ionization model (——) and a steady-state ionization model (---).

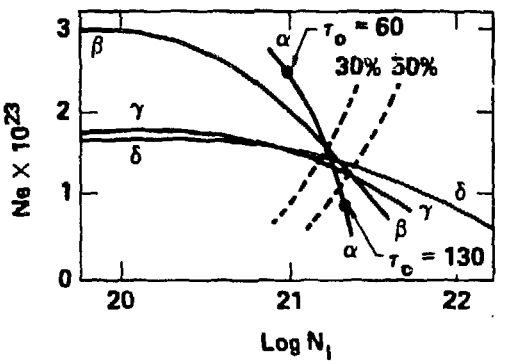

Fig. 3 Example of interpreting x-ray line broadening data to find imploded core densities. Ar-broadened Lyman series lines are fit to various electron densities, N_e, and ion densities, N_I. The intersection of the different curves determine the imploded core density. The dashed lines show the curves for when 30% and 50% of the total ion density are in the hydrogen-like ground state.